A stably expressed llama single-domain intrabody targeting Rev displays broad-spectrum anti-HIV activity

Eline Boons [a], Guangdi Li[b], Els Vanstreels[a], Thomas Vercruysse[a], Christophe Pannecouque[a], Anne-Mieke Vandamme[b,c], Dirk Daelemans[a*]

[a] Rega Institute for Medical Research, Laboratory of Virology and Chemotherapy, Department of Microbiology and Immunology, KU Leuven, Minderbroedersstraat 10, Leuven, B-3000, Belgium

[b] Rega Institute for Medical Research, Laboratory for Clinical and Epidemiological Virology, Department of Microbiology and Immunology, KU Leuven, Minderbroedersstraat 10, Leuven, B-3000, Belgium

[c] Centro de Malária e Outras Doenças Tropicais and Unidade de Microbiologia, Instituto de Higiene e Medicina Tropical, Universidade Nova de Lisboa, Lisboa 1349-008, Portugal

***** Corresponding author: Dirk Daelemans, Rega Institute for Medical Research, Laboratory of Virology and Chemotherapy, Department of Microbiology and Immunology, KU Leuven, Minderbroedersstraat 10, Leuven, B-3000, Belgium (+32 16 33 21 57)

E-mail addresses: Eline.boons@rega.kuleuven.be (Eline Boons), Guangdi.Li@rega.kuleuven.be (Guangdi Li), Els.vanstreels@rega.kuleuven.be (Els Vanstreels), Thomas.vercruysse@rega.kuleuven.be (Thomas Vercruysse), Christophe.pannecouque@rega.kuleuven.be (Christophe Pannecouque) Annemie.vandamme@uzleuven.be (Annemie Vandamme), Dirk.daelemans@rega.kuleuven.be (Dirk Daelemans)

Abstract

The HIV Rev protein mediates the transport of partially and unspliced HIV mRNA from the nucleus to the cytoplasm. Rev multimerizes on a secondary stem-loop structure present in the viral intron-containing mRNA species and recruits the cellular karyopherin CRM1 to export viral mRNAs from the nucleus to the cytoplasm. Previously we have identified a single-domain intrabody (Nb_{190}), derived from a llama heavy-chain antibody, which efficiently inhibits Rev multimerization and suppresses the production of infectious virus. We recently mapped the epitope of this nanobody and demonstrated that Rev residues K20 and Y23 are crucial for interaction while residues V16, H53 and L60 are important to a lesser extent.

Here, we generated cell lines stably expressing Nb_{190} and assessed the capacity of these cell lines to suppress the replication of different HIV-1 subtypes. These cells stably expressing the single-domain antibody are protected from virus-induced cytopathogenic effect even in the context of high multiplicity of infection. In addition, the replication of different subtypes of group M and one strain of group O is significantly suppressed in these cell lines. Next, we analysed the natural variations of Rev amino acids in sequence samples from HIV-1 infected patients worldwide and assessed the effect of Nb_{190} on the most prevalent polymorphisms occurring at the key epitope positions (K20 and Y23) in Rev. We found that Nb_{190} was able to suppress the function of these Rev variants except for the K20N mutant, which was present in only 0.7% of HIV-1 sequence populations (n=4632).

Cells stably expressing the single-domain intrabody Nb_{190} are protected against virus-induced cytopathogenic effect and display a selective survival advantage upon infection. In addition, Nb_{190} suppresses the replication of a wide range of different HIV-1 subtypes. Large-scale sequence analysis reveals that the Nb_{190} epitope positions in Rev are well conserved across major HIV-1 subtypes and groups. Altogether, our results indicate that Nb_{190} may have broad potential as a gene therapeutic agent against HIV-1.

Highlights

- The anti-Rev single-domain intrabody Nb_{190} displays broad-spectrum anti-HIV activity against different strains of both HIV-1 groups M and O.

- Nb_{190} was able to suppress the function of Rev mutants containing the most prevalent polymorphisms of the Nb_{190} epitope, except for the K20N mutant.

- Cells stably expressing Nb_{190} are protected against virus-induced cytopathogenic effect and display a selective survival advantage upon infection.

Keywords

HIV-1; single-domain antibody; intrabody; Rev

1. Introduction

HIV expresses three main RNA species, fully spliced, partially spliced and unspliced RNA, which encode for the regulatory, structural and viral enzymatic proteins. Various viral proteins are thus encoded by intron-containing mRNAs, which are naturally retained in the nucleus and degraded by host cell mechanisms. However, the nuclear export of these intron-containing viral mRNAs is crucial for viral replication (Pollard and Malim, 1998). To circumvent the nuclear retention and the degradation of these RNAs, HIV has developed a sophisticated mechanism. Through expression of the regulatory protein Rev, viral RNAs are hooked up to the cellular CRM1-mediated nuclear export pathway. Rev multimerizes on a secondary stem-loop structure, called Rev Responsive Element (RRE), present in all intron-containing viral RNAs (Fischer et al., 1999; Malim et al., 1989; Sodroski et al., 1986). This ribonucleoprotein complex is then exported to the cytoplasm via the CRM1-mediated nuclear export pathway (Neville et al., 1997). In the cytoplasm these RNAs serve as templates for translation into viral proteins and/or as genome for packaging into newly formed viral particles.

Structural analysis revealed that Rev consists of three major functional domains, (i) a nuclear localization signal (NLS) that also serves as RNA-binding domain and ensures binding of Rev to the RRE, (ii) a nuclear export signal (NES) that is essential for Rev to interact with the exportin CRM1 (Daelemans et al., 2005; Fischer et al., 1995; Neville et al., 1997) and (iii) two alpha helical multimerization domains that join together to form a head and tail multimerization surface, which is essential for the multimerization on the viral RNA (Jain and Belasco, 2001). During HIV replication, one Rev protein first binds to the RRE (stem IIB), facilitating dimerization via tail-tail interactions and further multimerization via both head-head and tail-tail interactions (Daly et al., 1989; Daugherty et al., 2008; Heaphy et al., 1990; Malim and Cullen, 1991; Vercruysse and Daelemans, 2014; Zapp et al., 1991). Subsequently,

the exportin CRM1 is recruited to this ribonucleoprotein complex, which exports viral RNA to the cytoplasm.

In previous research we have discovered a single-domain llama antibody (Nb_{190}) that interacts with the head multimerization surface of Rev. Nb_{190} inhibits the multimerization of Rev and supresses virus production from the HIV-1 NL4.3-molecular clone (Vercruysse et al., 2010; Vercruysse et al., 2011). Previously published crystal structures (Daugherty et al., 2010; DiMattia et al., 2010) allowed us to make an interaction model of Nb_{190} with Rev, disclosing the epitope of this nanobody and demonstrated that Rev residues K20 and Y23 are crucial for interaction while residues V16, H53 and L60 are important to a lesser extent (Vercruysse et al., 2013). However, the activity of this nanobody against different HIV-1 subtypes is not known.

Here, we have created cell lines that stably express Nb_{190} and show that these cells are resistant to the replication of HIV-1 subtype B. These Nb_{190} expressing cells display a selective survival advantage upon infection and were resistant to the replication of 7 different subtypes (subtype A, B, C, D, G and H) belonging to group M as well as a virus strain of group O, but not to a subtype F virus. Furthermore we analysed the natural variations of Rev amino acids occurring in sequence samples from HIV-1 patients worldwide and introduced the most prevalent polymorphisms of the key epitope residues (K20 and Y23) in wild-type subtype B Rev background. The binding of Nb_{190} to these Rev-mutants as well as its inhibitory activity on Rev function was assessed. Altogether, our study presents the first cell line stably expressing a nanobody with a broad-spectrum anti-HIV activity. Furthermore, Nb_{190} stable cells display a selective survival advantage upon infection.

2. Materials and Methods

2.1 Production of stable cell lines

For the generation of stable cell lines, HEK293T cells were transfected using the calcium phosphate method with 8 µg pCGGagPol, 2 µg of pCF-VSVG and 10 µg of pQ-puroR-Nb_{190}(mKO)FLAG or pQ-puroR-Nb_{163}(mKO)FLAG (Ulm et al., 2007). Cells were grown overnight at 37 °C, washed and fresh medium was added. The next day, supernatant was harvested, spun down to remove residual cells and was added to C8166, HeLaP4 or U87CD4CCR5 cells with 8 µg/mL hexadimethrine bromide. After 2 days, cells were subject to selection by 2 µg/mL puromycin. Surviving cells were kept in culture for at least 1 week before use and monitored under fluorescence microscope and western blot analysis was used to confirm maintenance of the insert of interest.

2.2 Transfections and Plasmids

HeLa cells, maintained using standard procedures, were transfected with plasmid DNA using the transfection reagent Genecellin, according to the manufacturers protocol. For the co-localisation experiment 0.1 µg of pRev-AcGFP and 0.2 µg pcDNA3.1 Nb_{190}-mKO or Nb_{163}-mKO after 1 h the cells were washed with Phosphate Buffered Saline (PBS) and fresh medium was added. The day after, transfected HeLa cells were imaged. For the analysis of the stable cell lines, HeLaP4 or U87CD4CCR5 cells were transfected with pRev-AcGFP using Genecellin as described above. Because C8166 could not be transfected with Genecellin, co-transduction was carried out. Protocol was analogous to the production of stable cell lines; except for the insert of interest that now was Rev-AcGFP. After 2 days, cells were imaged with a SP5 laser-scanning confocal microscope (Leica Microsystems), using an HCX plan apochromat x63 (numerical aperture 1.2) water immersion objective magnification. Monomeric *Aequorea coerulescens* green fluorescent protein was monitored with the argon laser using the 488-nm line for excitation, and emission was detected between 495 nm and

550 nm. Monomeric Kusabira-Orange fluorescent protein (mKO) was imaged using the DPSS 561-nm laser for excitation, and emission was detected between 570 nm and 670 nm.

For the rescue experiment HeLaP4 cells, whether or not stably expressing Nb_{190}-FLAG or Nb_{163}-FLAG, were co-transfected with 0.5 µg Rev-AcGFP or mutant Rev-AcGFP and 0.5 µg pHIV Mrev(-) using the transfection reagent Genecellin, according the manufacturers protocol. After one day, supernatant was collected and virus-associated capsid protein (p24) was determined by an enzyme-linked immunosorbent assay (Perkin Elmer).

Site-directed mutagenesis was performed by methylation of the parental DNA by the GpC methyltransferase (New England Biolabs) followed by PCR using the Platinum Taq DNA polymerase (Invitrogen) and primers containing the target mutations, this according to the manufacturers protocol.

Cloning of the viral Bz163- and BaL- *rev* gene was performed as follows. Briefly, RNA was isolated out of infected cells with the RNeasy micro-kit (Qiagen, 74004). Reverse transcription of the isolated RNA to DNA was performed with the Superscript III one-step RT-PCR (Invitrogen) according to the manufacturers protocol. Afterwards this DNA was cloned into the pAcGFP-N1 vector.

2.3 Infection

C8166 and U87CD4CCR5 cells were maintained using standard procedures. In the medium of stable cells, 1 µg/mL puromycin was added. C8166 cells were incubated with X4-viruses III_B (Subtype B), UG270 (Subtype D) and BCF06 (Group O). U87CD4CCR5 were infected with R5-viruses UG275 (Subtype A), ETH2220 (Subtype C), Bz163 (Subtype F), BcFDioum (Subtype G) and BcFKita (Subtype H) at an MOI of 0.1; 0.01; 0.001; 0.0001 or 0. Cells were washed 3 times with PBS and resuspended in medium 1 h or 24 h post-infection, respectively. Five days post-infection supernatant was collected and virus-associated core antigen (p24)

was determined by an enzyme-linked immunosorbent assay (Perkin Elmer) according to the manufactures protocol. Cell viability was determined with the MTT-method. The absorbances were read in an eight-channel computer-controlled photometer (Infinite M1000, Tecan), at two wavelengths (540 and 690 nm) as described previously (Pannecouque et al., 2008; Pauwels et al., 1988). For determination of selective growth advantage, C8166 co-cultures containing different ratio (25:75; 50:50 or 75:25) of $C8166_{Nb190}$ cells with either wild-type or $C8166_{Nb163}$ cells were infected with HIV-1 III_B at different MOI. Cell survival was assessed by MTT 5 days post infection.

For the production of NL4.3-CTE virus, the corresponding plasmid (from B. Felber and G. Pavlakis) was transfected in HEK293T cells. After 24 h medium was replaced and another 24 h later supernatant was harvested. C8166 or U87CD4CCR5 cells were infected with 200, 40 and 8 pg virus (expressed as p24 and determined by p24 ELISA). Supernatant was harvested after 5 days and p24 was determined as described above.

2.4 Co-immunoprecipitation

HeLa cells were transfected with pRev-AcGFP and collected after 18 h. Next to that $1x10^6$ HeLaP4, C8166 or U87CD4CCR5 stable cells were collected and lysed in a 0.5 % triton lysis buffer (50 mM NaCl, 5 mM MgCl and 50 mM Tris HCl) for 1 h on ice. The lysates were cleared of debris by centrifugation and supernatant of transfected cells was co-incubated with lysate of the stable cell line cells together with Sigma anti-FLAG M2 magnetic beads for 1 h at 4 °C. Beads were washed 3 times with wash buffer (50 mM NaCl, 5 mM MgCl and 50 mM Tris HCl). Afterwards NuPage LDS sample buffer (Life Sciences) was added together with DTT and samples were kept at 80 °C for 5 min in order to elute proteins from beads. Proteins were analysed by Western Blotting, visualising Nanobody-FLAG fusion proteins with Mouse anti-FLAG (F1804, Sigma-Aldrich) and Rev with rabbit anti-Rev (20-000501, Fitzgerald).

Secondary antibodies were Goat anti-mouse IgG-HRP (sc-2005 Santa Cruz) or Donkey pAb to Rabbit IgG (Abcam 9764), respectively.

2.5 Fluorescence Recovery after Photo bleaching

Fluorescence recovery after photo-bleaching studies were performed by obtaining a series of 20 pre-bleach images of a nucleolus at 5% Acousto optical tunable filter laser setting, followed by a single 0.39 s bleach iteration at full laser power of a 1 μm wide circle in the nucleolus. Subsequent post-bleach images were acquired at 5% Acousto optical tunable filter with the following time scheme: 20 images every 0.39 s, 20 images every 1 s, and 15-55 images every 10 s. Data were background-subtracted, bleach-corrected and normalized according to the method described in (McNally, 2008). Half times of recovery were obtained by fitting the recovery curves employing GraphPad Prism (GraphPad Software, Inc.).

2.6 Sequence conservation analysis

We retrieved 6346 HIV-1 Rev sequences from the HIV Los Alamos database (http://www.hiv.lanl.gov). Only one sequence per patient sample was included. We aligned sequences against the HXB2 reference and manually curated using Seaview 4.3 (Gouy et al., 2010). Hypermutated sequences were detected by the Los Alamos hypermut tool (default parameters) (Rose and Korber, 2000). HIV-1 subtype classification was determined using the Rega (Pineda-Pena et al., 2013) and COMET subtyping tools (http://comet.retrovirology.lu/). Sequence quality was ensured by excluding duplicates and sequences with internal stop-codons, hypermutations, more than 1% ambiguous nucleotides and discordant subtype classification. We obtained 4632 full-length HIV-1 Rev sequences that fulfilled the quality criteria, encompassing A1 (n = 177), B (n = 2701), C (n = 1027), D (n = 106), F1 (n = 25), F2 (n = 8), G (n = 57), H (n = 4), J (n = 3), K (n = 2), CRF01_AE (n = 409), CRF02_AG (n =

91), group O (n = 6), group P (n = 2), group N (n = 9). To quantify the statistical conservation of amino acids at each Rev position, conservation index (CI) was calculated by averaging pairwise scores between all AAs using the BLOSUM62 substitution matrix (Li et al., 2013). The HIV-1 Rev inter- and intra-subtype diversity was calculated using the pairwise sequence comparison, described in our recent study (Li et al., 2013) (Table 1).

Sequences from lab-strains were obtained from http://www.hiv.lanl.gov/cgi-bin/NEWALIGN/align.cgi.

3. Results

3.1 Cell lines stably expressing Rev-binding Nb_{190}

We have previously shown that Nb_{190} inhibits virus production from HEK293T cells that were transfected with the NL4.3 molecular clone (subtype B) (Vercruysse et al., 2010). However, the effect of Nb_{190} on virus infection or its effect on different HIV-1 subtypes has not been assessed. Therefore we created C8166, U87CD4CCR5 and HeLaP4 cell lines, which stably express Nb_{190}, the Nb_{190}-mKO fusion protein or the negative control nanobody Nb_{163} or the Nb_{163}-mKO fusion protein.

To test the activity of the stably expressed Nb_{190} and its ability to interact with Rev, the cytoplasmic relocalization of Rev-AcGFP in the presence of Nb_{190} was monitored. Wild-type Rev is predominantly localized in the nucleoli of the cells (Kalland et al., 1994; Meyer and Malim, 1994). Nevertheless we have shown that interaction of Nb_{190} with Rev inside living cells causes a redistribution of both proteins to the cytoplasm (Vercruysse et al., 2010). This localization pattern is in line with the subcellular localization of Rev mutants that are unable to multimerize (Daelemans et al., 2004; Jain and Belasco, 2001; Malim and Cullen, 1991; Thomas et al., 1998). In $HeLaP4_{Nb190}$, $C8166_{Nb190}$ and $U87CD4CCR5_{Nb190}$ cells, transiently expressed Rev-AcGFP localizes in the cytoplasm. In $HeLaP4_{Nb190\text{-}mKO}$, $C8166_{Nb190\text{-}mKO}$ and

U87CD4CCR5 $_{Nb190\text{-}mKO}$ cell lines expressing the Nb_{190}-mKO fusion protein, both Rev-AcGFP and Nb_{190}-mKO redistribute to the cytoplasm (Fig. 1 A, B and C). These results demonstrate that the stably expressed intrabody Nb_{190} interacts with Rev in the stable cell lines. As a control, relocalization of Rev-AcGFP to the cytoplasm was absent in cells expressing the negative control Nb_{163} nanobody (Fig. 1 A, B and C). These results indicate that the fusion of mKO to the nanobody does not affect its activity. The interaction of Nb_{190} with Rev in these cell lines was confirmed by co-immunoprecipitation of Rev with Nb_{190} (Fig. 2).

3.2 Nb_{190} suppresses the replication of different HIV-1 subtypes

Next we assessed the replicative capacity of different HIV-1 subtypes in these cell lines stably expressing Nb_{190}. We first assessed the replication of HIV-1 subtype B strain III_B in these cells. Therefore, $C8166_{Nb190}$ cells were infected with HIV-1 III_B at different multiplicities of infection (MOI) and virus replication was monitored 5 days post infection by measuring the virus-induced cytopathogenic effect (CPE) using MTT (Pannecouque et al., 2008) (Fig. 3A) as well as the virus-associated p24 in the supernatant (Fig. 3B). CPE was strongly suppressed in Nb_{190} expressing cells and the replication of III_B was strongly inhibited as compared to wild-type or Nb_{163} expressing cells. In fact, at an MOI of 0.01, virus replication was fully blocked in Nb_{190} expressing cells whereas Nb_{163} expressing or wild-type C8166 cells produced 1.6×10^5 pg/mL and 1.0×10^5 pg/mL virus-associated p24, respectively. To prove that the observed protection against viral replication is not due to eventual defects in cellular machineries caused by the stable insertion of the Nb_{190} in the cellular genome, replication of a Rev-independent virus (NL4.3-CTE) (Bray et al., 1994; Sonigo et al., 1986; Zolotukhin et al., 1994) was assessed in these stable cell lines (Vercruysse et al., 2010). This Rev-independent virus relies on the Constitutive Transport Element (CTE) of the Mason-Pfizer monkey virus

for the nuclear export of its intron-containing mRNAs and is therefore not inhibited by Nb_{190} (Bray et al., 1994; Sonigo et al., 1986; Zolotukhin et al., 1994). NL4.3-CTE virus was able to replicate in our stable cell lines (Fig. 4) suggesting that the stable introduction of the intrabody sequence as such does not affect steps in the viral replication other than the Rev function. Moreover, these results again confirm the strict anti-Rev activity of Nb_{190}.

To further determine whether Nb_{190} was able to suppress replication of other HIV-1 subtypes, infection of $C8166_{Nb190}$ and $U87CD4CCR5_{Nb190}$ cells was performed with respectively different X4- or R5-strains (Fig. 5A-B). We assessed viral replication in C8166 cells by both virus-induced CPE (using MTT) and virus release in the supernatant (p24 ELISA). For U87CD4CCR5 cells, we only assessed virus-associated p24 in the supernatants, as these cells are less prone to expressing CPE. Interestingly, the replication of all viruses tested was inhibited, except for subtype F (Bz163) (Table 2). Overall, these experiments demonstrate that Nb_{190} is able to suppress viral replication of different HIV-1 subtypes, and that cells stably expressing Nb_{190} are protected from virus-induced cytopathogenic effects.

3.3 Selective survival advantage of cells stably expressing Nb_{190}

As Nb_{190} stable cell lines are resistant to CPE induction upon HIV-1 (III_B) infection (Fig. 3A), we investigated whether they have a selective survival advantage compared to wild-type or the control Nb_{163} stable cell lines upon infection. Therefore C8166 co-cultures containing different ratio (25:75; 50:50 or 75:25) of $C8166_{Nb190}$ cells with either wild-type or $C8166_{Nb163}$ cells were infected with HIV-1 III_B at different MOI and cell survival was assessed by MTT 5 days post infection. Results show that the higher the percentage of Nb_{190} expressing cells, the more viral particles were required to induce cell death by HIV-induced cytopathogenic effect (Fig. 6). Indeed, there is a clear correlation between the percentage of stable Nb_{190} cells and the amount of cell survival upon infection at a certain MOI.

3.4 Analysis of Rev sequence variations at the Nb_{190} epitope positions in large-scale HIV-1 patient populations

Previously we have shown that Rev residues V16, K20, Y23, H53 and L60 interact with Nb_{190}. Mutation of these residues to an alanine resulted in a decreased binding affinity of Nb_{190} (Vercruysse et al., 2013). Because of the high sequence variations in HIV, we analysed the Rev sequences from viruses of 4632 patients worldwide and quantified the conservation index of the epitope residues V16, K20, Y23, H53 and L60 (Fig. 7 A and B). Despite 16.16% genetic diversity of HIV-1 Rev within subtype strains, 25.94% between subtypes and 52.94% between group strains, we found that V16, K20, Y23, and L60 are well conserved across major HIV-1 subtypes; however H53 was much less conserved (Fig. 7 B, C, Fig. 8 and 9). Notably, natural polymorphisms at residues K20 and Y23 were prevalent in less than 7% across HIV-1 subtypes (K20R: 5%, K20N: 0.7% or Y23H: 0.8%; Fig. 7 C).

As we already established that K20 and Y23 are the most important epitope residues, we decided to introduce the most frequently observed polymorphisms at those positions (K20R, K20N, and Y23H mutations) into the subtype B background Rev and investigated whether these mutations could affect the interaction of Nb_{190} with Rev. We therefore co-transfected these Rev-AcGFP-mutants together with Nb_{190}-mKO and monitored their subcellular localization as described above (Fig. 10 A and B). Wild-type Rev-AcGFP normally localizes to the nucleoli while in the presence of Nb_{190}-mKO both proteins relocalize to the cytoplasm suggesting interaction between both proteins (Vercruysse et al., 2010). Unlike wild-type Rev-AcGFP, the Rev-AcGFP-Y23H and Rev-AcGFP-K20N mutants already localize in the cytoplasm in the absence of Nb_{190} (Fig. 10 B). However, upon co-expression of the labelled Nb_{190}-mKO fusion protein with Rev-AcGFP-Y23H, Nb_{190}-mKO redistributed to the cytoplasm suggesting that Nb_{190} is able to interact with the Rev-Y23H mutant. Rev-AcGFP-

K20N was unable to cause a redistribution of Nb_{190}-mKO suggesting that the K20N mutation abolishes the Rev-Nb_{190} interaction. To our surprise, the K20R Rev mutant, which localizes to the nucleoli in the absence of Nb_{190}, did not redistribute to the cytoplasm in the presence of Nb_{190}, but Nb_{190}-mKO redistributed to the nucleoli suggesting interaction of both proteins.

To confirm the above findings, we measured the affinity of Nb_{190} to these Rev mutants using Fluorescence Recovery After Photo bleaching (FRAP). Therefore, Nb_{190}-mKO was co-transfected with RevM10-AcGFP containing one of the mutations. RevM10-AcGFP lacks a nuclear export signal (NES) and hence does not shuttle to the cytoplasm but localizes in the nucleoli even in the presence of Nb_{190}. After bleaching of Nb_{190}-mKO within a 1µm diameter circle in the nucleoli, its reappearance was measured in time. Recovery curves of Nb_{190}-mKO bound to RevM10K20R or RevM10Y23H were similar to the one of RevM10 indicating that Nb_{190}-mKO binds with comparable affinity to these proteins. However, a very fast recovery of Nb_{190}-mKO was observed when bound to RevM10K20N, suggesting a very weak affinity (Fig. 11 A).

To further investigate whether Nb_{190} can inhibit the function of these Rev mutants in virus replication, we co-transfected $HeLaP4_{Nb190}$ cells with a Rev deficient NL4.3 molecular clone containing a stop codon in its *rev* gene together with wild-type Rev or Rev containing the K20R, K20N or Y23H mutations in wild-type background. Virus production from the Rev-deficient NL4.3 clone is rescued by co-expression of Rev protein. Nb_{190} was able to suppress virus production from all Rev mutants except for RevK20N (Fig. 11 B). Remarkably, this mutant displayed a decreased functionality.

3.4 Analysis of Bz163-resistance to Nb_{190}

To further investigate the resistance of Bz163 against Nb_{190}, we introduced the amino acid variations of Bz163-Rev located in the Nb_{190}-epitope (V16A and H53R) into wild-type

subtype B background Rev. We co-transfected HeLaP4$_{Nb190}$ cells with a Rev deficient NL4.3 molecular clone together with wild-type Rev or Rev containing the V16A, H53R or V16A-H53R mutations. Virus production was rescued in HelaP4 and HelaP4$_{Nb163}$ cells by both wild-type as mutant Rev protein and Nb_{190} was able to inhibit the virus production induced by all single - and double mutants of Rev (Fig. 12 A).

Because the above experiments did not elucidate the cause of resistance of strain Bz163, we cloned the Rev of Bz163 *via* reverse genetics into an expression vector and three different clones were tested in the same rescue experiment as described above. As a control also two Rev-clones of BaL were tested. The Rev proteins of both Bz163 and BaL were able to support virus production and Nb_{190} was able to inhibit this virus production (Fig. 12 B).

4. Discussion

HIV still affects millions of people worldwide and a curative therapy has not been established to date. The emergence of resistant viruses and side effects of long-term combination therapy directs science towards the development of new possible therapies (Barre-Sinoussi et al., 2013). For example, nanobodies are small, soluble and non-immunogenic agents with high target binding capabilities (Muyldermans et al., 2001; Pardon et al., 2014; Siontorou, 2013). Several nanobodies have been under investigation in clinical phases for diverse applications such as the treatment of acquired thrombotic thrombocytopenic purpura and several cancers (Callewaert et al., 2012; Holz, 2012; Oliveira et al., 2013). Recently, we have discovered a nanobody (Nb_{190}) that inhibits the multimerization of the HIV Rev protein and doing so suppresses the production of virus (Vercruysse et al., 2010; Vercruysse et al., 2011). It is the first inhibitor of its kind and it may have potential as a gene therapeutic agent against HIV. For long time the crystal structure of Rev remained unsolved due to the strong propensity of Rev to aggregate in solution. However, introduction of point mutations in the multimerization

domains (Daugherty et al., 2010) or the use of agents that reduce oligomerization (DiMattia et al., 2010; Stahl et al., 2010) allowed the elucidation of Rev's structure. It became clear that the hydrophobic amino acids V16 and L60 are located at the outer surface of an alpha-helix and that they both play a direct role in the multimerization of Rev by forming key stabilizing interactions. The polar residue Y23 participates in interactions within the monomer Rev and bridges interactions with the second Rev molecule in the dimer-formation. The 3D-structure of the Rev dimer further provided detailed information on the position of the amino acids at the surface of this multimerization domain. This formed the basis for a thorough structural analysis of the binding interaction to elucidate the forces driving dimerization and higher-order multimerization of the Rev protein (Venken et al., 2012). This information combined with the results of our previous experiments allowed us to make an interaction model of Nb_{190} binding at the head multimerization domain of Rev disclosing the amino acids that play an important role in the interaction between Rev and Nb_{190}, being V16, K20, Y23, H53 and L60 (Vercruysse et al., 2013).

In the current study we investigated the broad-spectrum anti-HIV activity of Nb_{190} by means of cell lines that stably express this nanobody. We could not detect any cytotoxicity or negative effect on cell proliferation over months of cell culturing in these cell lines stably expressing the nanobody. Furthermore in contrast to wild-type C8166 cells, cells stably expressing Nb_{190} were resistant for viral replication and survived infection with virus. In Nb_{190} expressing cell lines replication of HIV-1 subtype A, B, C, D, G, H and group O is severely impaired. One exception was subtype F (Bz163) that is insensitive to Nb_{190}; nevertheless this subtype accounts for only 0.45% of the global number of HIV-1 infections worldwide (Abecasis et al., 2013; Hemelaar et al., 2011). Sequence analysis of subtype F strain Bz163 revealed that this virus contains two amino acid variations (V16A and H53R) in the epitope of the Rev protein (Table 3). Analysis of 4632 patient samples (Figure 7 and 8)

revealed that only 0.8% of the Rev sequences contain an alanine at position 16 (subtype B and C) whereas 77% (subtype B, C, G, F and H) of the patient samples contain an arginine instead of a histidine residue at position 53. Double mutants (V16A-H53R) occurred in less than 0.8% of the HIV-1 patient population. Similar dual variations (V16I and H53D) were found in UG275 (subtype A) and BcF06 (group O) viruses. Although Nb_{190} was able to suppress replication of these viruses, they were less sensitive than the III_B strain (Fig. 5 and Table 2). Variations in just one amino acid residue at positions V16 or H53 did not strongly affect the inhibition by Nb_{190} (see BaL, BcFDioum or BcFKita, Table 2 and 3). These findings suggest that the combination of at least two mutations in these epitope hot spot positions of Rev severely decreases or abolishes the inhibitory activity of the nanobody. Further in depth investigation of the resistance of Bz163 towards Nb_{190} led to an interesting observation. We first introduced V16A, H53R and V16A-H53R double mutations into the subtype B Rev background and investigated whether these mutations could account for the observed resistance profile. Rescue experiments revealed that Nb_{190} could still inhibit the Rev function from these subtype B mutants (Fig. 12 A). Therefore, in a next step we subcloned the full Bz163 Rev sequence *via* reverse genetics into an expression vector and three different clones were tested in the same rescue experiment (Fig. 12 B). In this setup the nanobody was still able to inhibit the function of Bz163 Rev. Therefore, resistance of Bz163 to Nb_{190} could not be explained by site directed mutagenesis or reverse genetics and future research will further have to explore the mechanism of the observed resistance.

To further predict the inhibitory potential of Nb_{190} against HIV-1 viruses prevailing amongst patients, we examined the prevalence of the important epitope residues using a large-scale dataset with Rev sequences sampled from 4632 HIV-1 patients (Fig. 7C and Fig. 8). The key epitope residues K20 and Y23 (Vercruysse et al., 2013) are well conserved across the HIV-1 population. For K20 only 5 % of the viruses contain R and 0.7% contain N at this position,

whereas only 0.8% of the viruses varied at position 23 (Y to H). To investigate the effect of these specific Rev variations on the activity of Nb_{190}, we introduced mutations (K20R, K20N or Y23H) into a Rev subtype B background. The K20R and Y23H mutations did not affect the binding with Nb_{190} while K20N dramatically decreased the affinity of Nb_{190}. These observations may be explained by the fact that a lysine to asparagine mutation (K20N) causes a change from positively charged to polar propensities. Mutation of lysine to arginine (K20R) on the other hand preserves the long side chain and charge for interactions with the Nb_{190} residues, T33, Y105 and D107 (Vercruysse et al., 2013). Also, mutation of a tyrosine to histidine (Y23H), does not introduce dramatic change of residue size and histidine can still engage in a π-π interaction with the F100 residue of Nb_{190} (Vercruysse et al., 2013).

Altogether, a broad analysis of patient samples combined with a variety of experimental data demonstrates that Nb_{190} displays a broad-spectrum anti-HIV-1 activity. Although nanobodies have good potential as drug molecules we do believe that, because of the intracellular localisation of the target, intravenous application of Nb_{190} as anti-HIV agent in the clinic is not likely unless future developments in the nanobody research field would allow its entry into cells. As such the nanobody will not enter the cell, and additional modifications (such as membrane permeable peptides) might be required to make a nanobody that permeates the cell membrane. In contrast, Nb_{190} may be further developed for gene therapeutic strategies involving the transduction of T-cells to generate immune systems resistant to HIV infection (Anderson and Akkina, 2008; Zhen and Kitchen, 2014). Therefore in future studies we will study it in Primary Blood Monocytic cells and initiate in viral resistance studies. Secondly Nb_{190} can stand as a model for drug discovery efforts in future studies.

5. Conclusion

In conclusion, we show that a single-domain llama antibody that inhibits the multimerization of the HIV Rev protein can be stably expressed in different cell lines. Interestingly, these cells are protected from virus-induced cytopathogenic effect even at high multiplicity of infection. In addition this single-domain antibody displays broad-spectrum anti-HIV-1 activity. Sequence analysis revealed that the epitope residues are largely conserved across different major HIV-1 subtype strains. We conclude that this nanobody may have potential for further development as gene therapeutic agent.

Figures

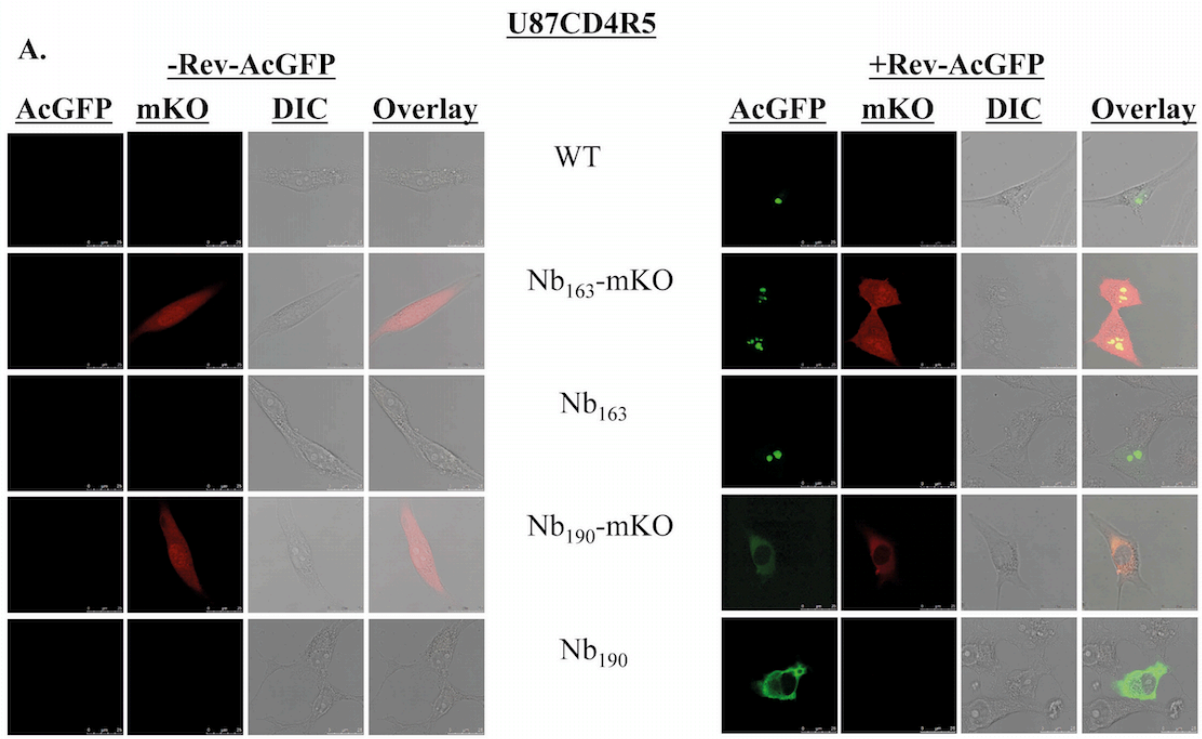

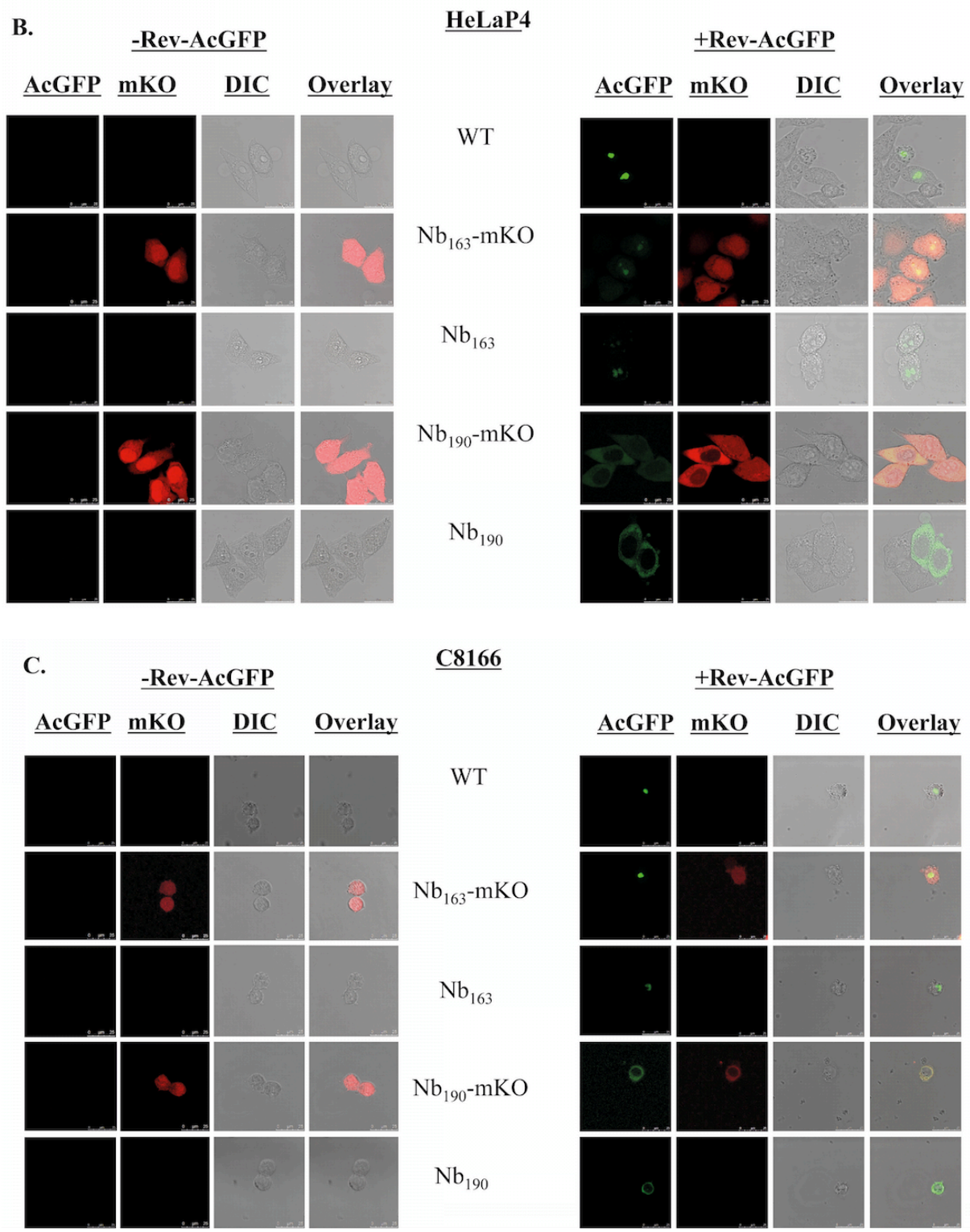

Fig. 1 Co-expression of Rev and Nb_{190} results in a relocalization of both Nb_{190} and Rev

(A) U87CD4CCR5 or **(B)** HeLaP4 cells stably expressing the negative control Nb_{163}(mKO) or the active Nb_{190}(mKO) were transfected with Rev-AcGFP. GFP (green) and mKO (red)

were visualized using confocal fluorescence microscopy. The third column shows differential interference contrast (DIC).

(C) C8166 cells stably expressing the negative control Nb_{163}(mKO) or the active Nb_{190}(mKO) were transduced with a vector expressing Rev-AcGFP. GFP (green) and mKO (red) were visualized using confocal fluorescence microscopy. The third column shows differential interference contrast (DIC).

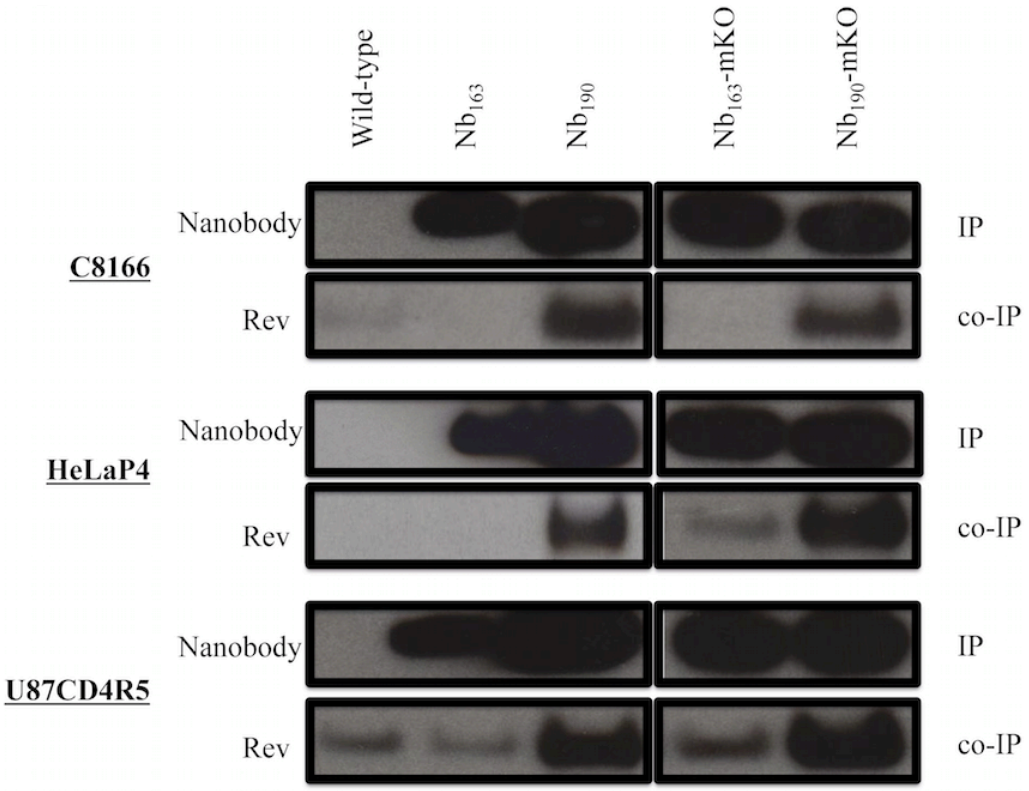

Fig. 2 Nb_{190} interacts with Rev in Nb_{190} expressing stable cell lines as demonstrated by co-immunoprecipitation

Lysate of HeLa cells transfected with Rev-AcGFP was mixed with lysate of wild-type (C8166, HeLaP4, U78CD4R5) cells or cells stably expressing Nb_{190}(mKO) or the negative control Nb_{163}(mKO). Nanobodies (bait, IP) with the bound Rev (prey, co-IP) were pulled-down out of the mixture using coated magnetic beads. Presence of nanobody (IP) and/or Rev (co-IP) in the pull-down was visualized by western blotting.

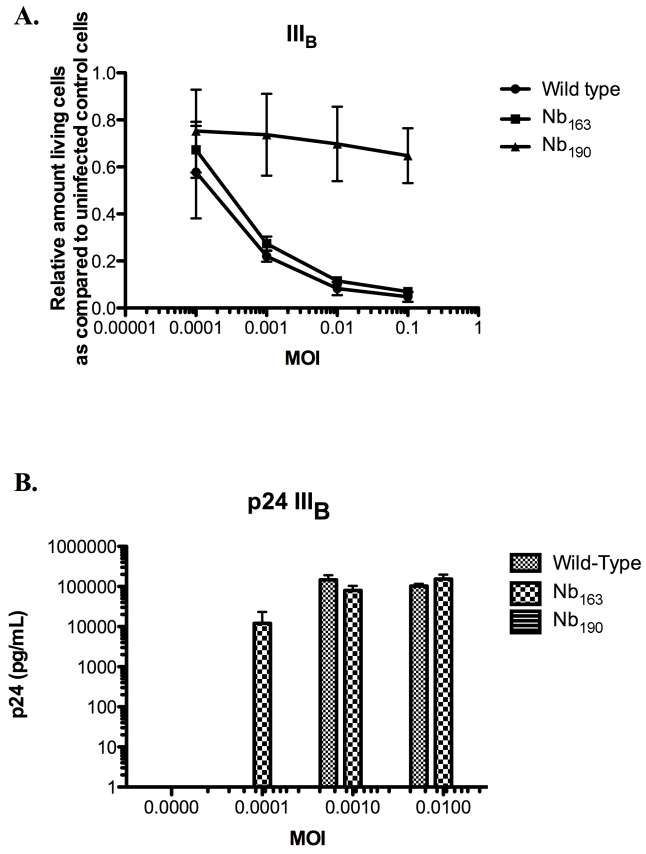

Fig. 3 Stably expressing Nb_{190} cell lines are resistant to HIV-1 III_B replication and are protected from CPE

C8166 stable cell lines were infected with HIV-1 (III_B) at different multiplicities of infection (MOI). Five days post infection, cell viability was assessed using MTT **(A)** and virus replication was assessed by quantification of the virus-associated p24 in the supernatant of infected cell cultures **(B)**. Average of 3 independent experiments with standard deviations (SD) are shown.

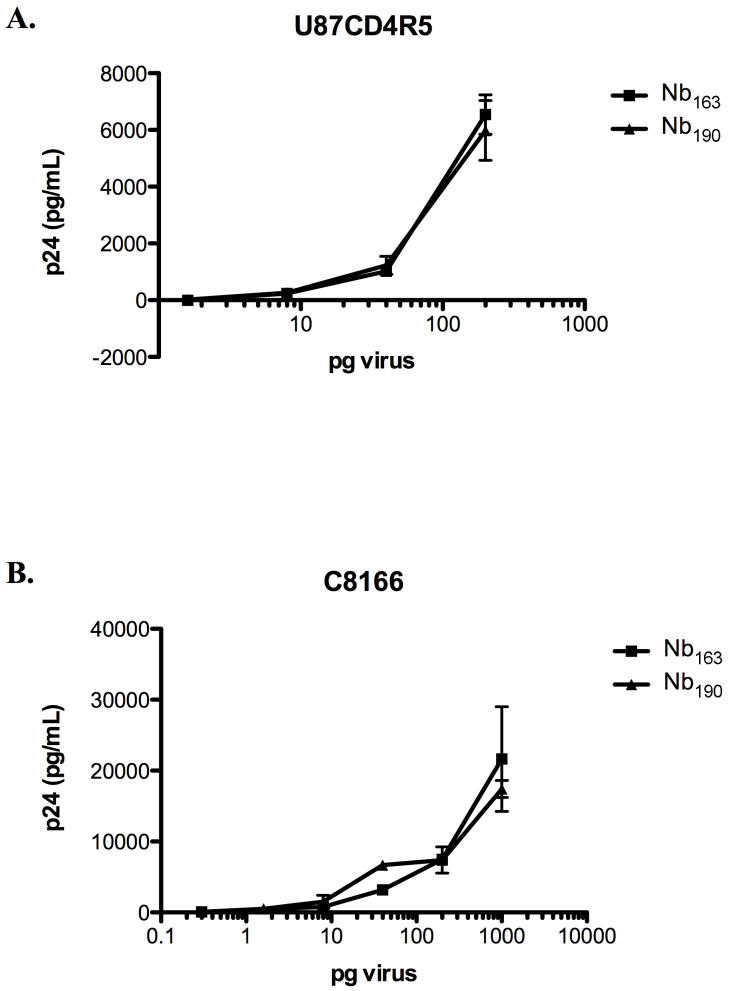

Fig. 4 Stable expression of Nb_{190} does not affect the replication of Rev-independent virus

U87CD4CCR5 and C8166 stable cells were infected with NL4.3-CTE virus and p24 was measured after 5 days. X-axis is showing the input amount of p24 (pg/mL). Average of 3 independent experiments with SD are shown.

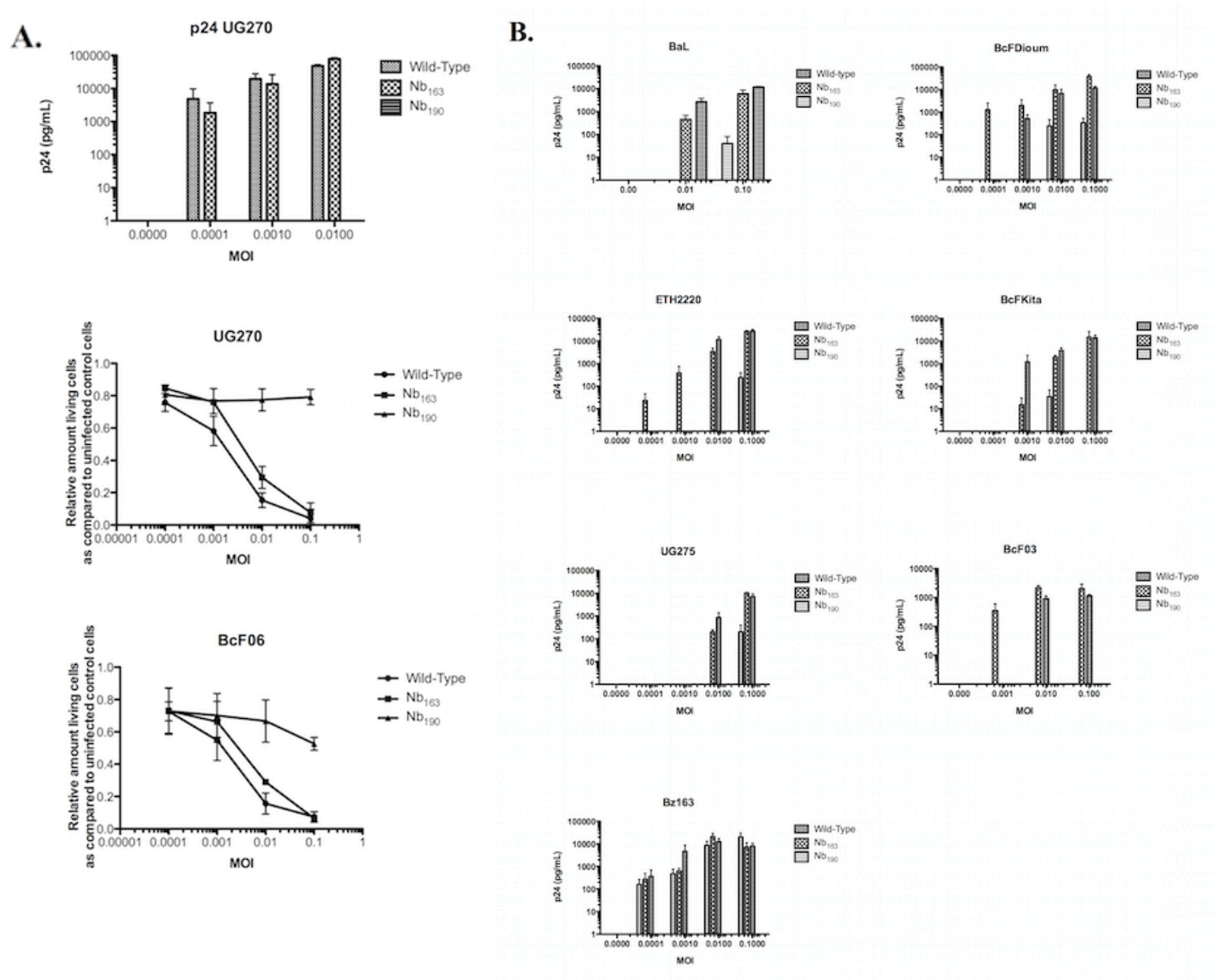

Fig. 5 Nb_{190} displays broad-spectrum anti-HIV activity

(A) Nb_{190} or Nb_{163} expressing C8166 cells or wild-type C8166 cells were infected with HIV-1 strains UG275 or BcF06 at different multiplicities of infection (MOI). One hour post infection cells were washed and further cultured at 37°C. Virus induced CPE using MTT and p24 in the supernatant were determined 5 days post infection. For BcF06, only MTT-method was used. Average of 3 independent experiments with SD are shown.

(B) Nb_{190} or Nb_{163} expressing U87CD4CCR5 cells or wild-type U87CD4CCR5 cells were infected with R5-viruses BaL, ETH2220, UG270 Bz163, BcFDioum, and BcFKita. The

amount of virus-associated p24 in the supernatant was determined by ELISA 5 days post infection. Average of 3 independent experiments with SD are shown.

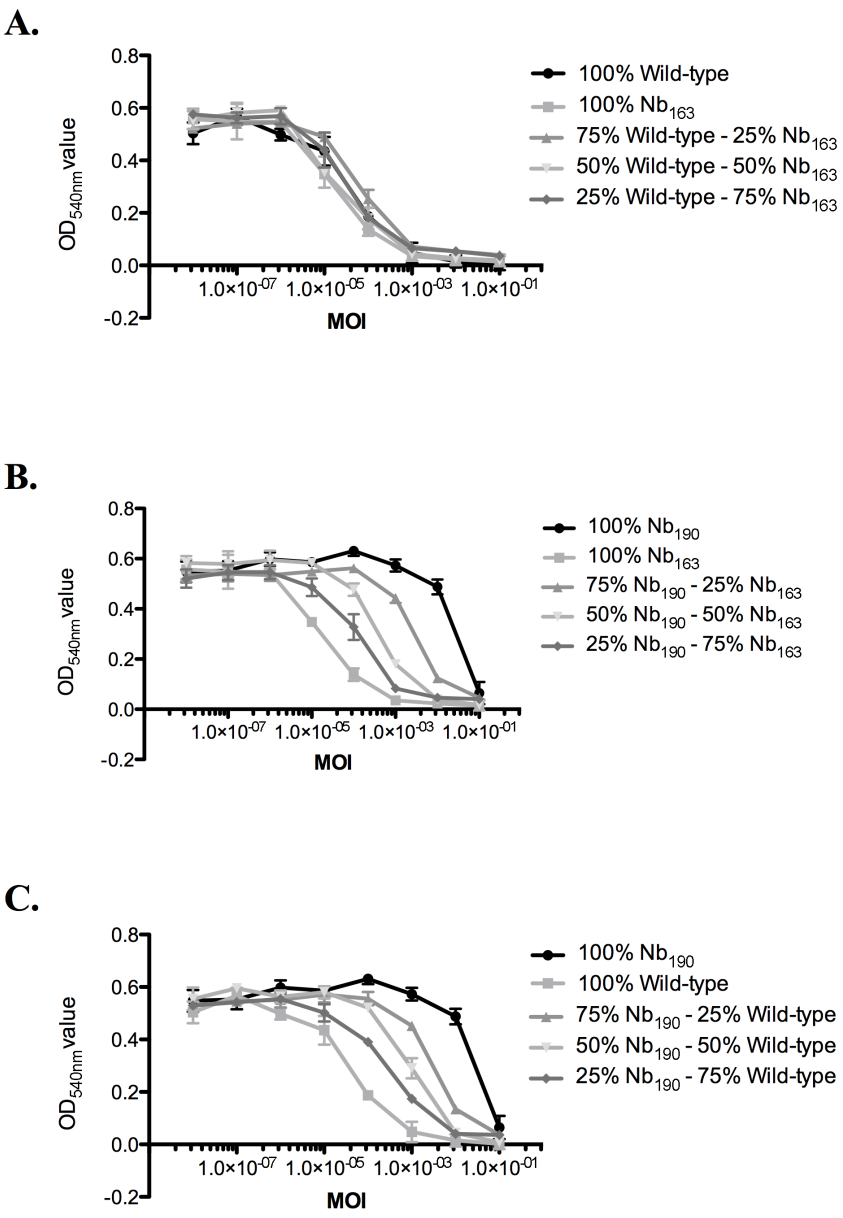

Fig. 6 C8166 Nb_{190} cells display a selective growth advantage upon HIV-1 infection

Co-cultures of different amounts of (**A**) wild-type C8166 cells with $C8166_{Nb163}$ stable cell lines or **(B)** $C8166_{Nb163}$ with $C8166_{Nb190}$ stable cell lines or **(C)** wild-type C8166 cells with $C8166_{Nb190}$ stable cell lines were infected with HIV-1 III_B virus at different MOI. Five days post infection cell viability was assessed with the MTT-method. Average of 3 independent experiments with SD are shown.

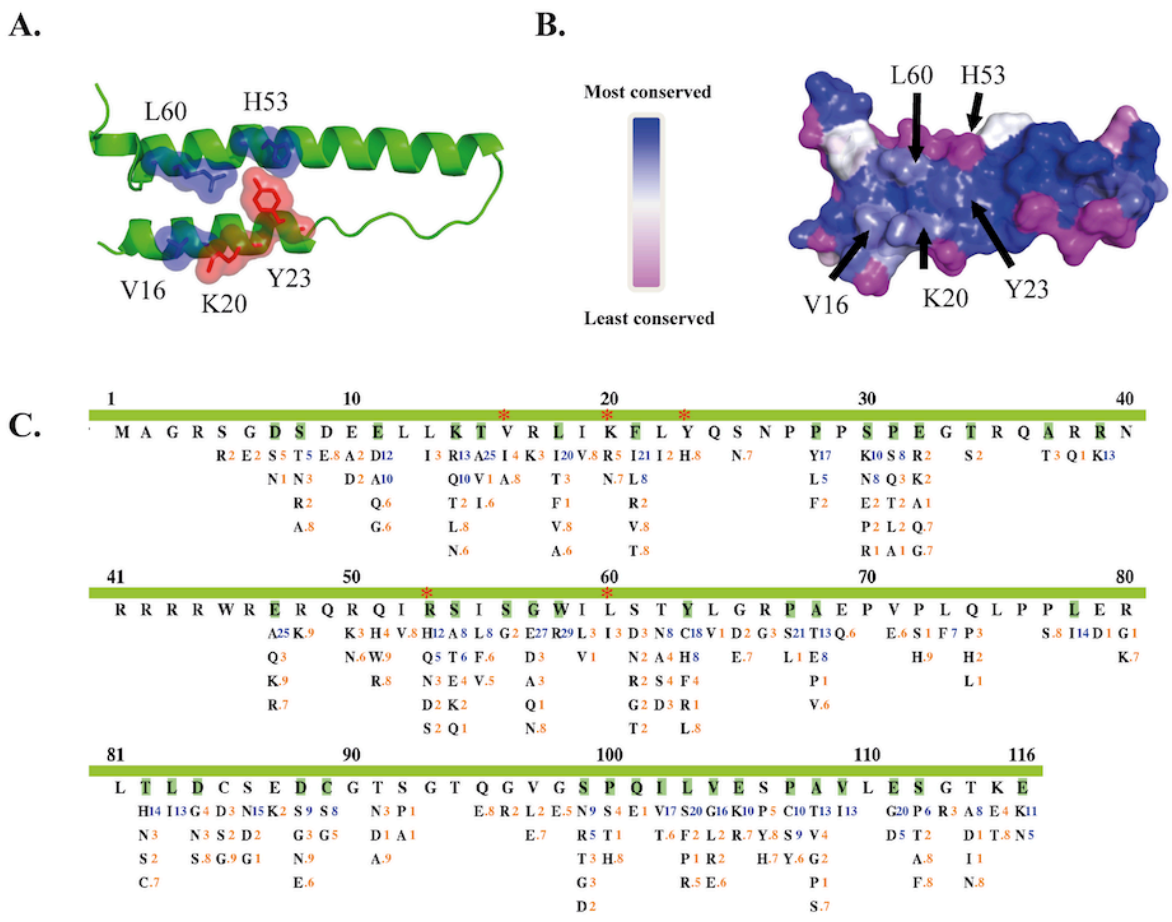

Fig. 7 Sequence analysis of epitope residues in Rev among 4632 viral strains

(A) Protein interaction positions are mapped onto Rev protein structure.

(B) Surface spectrum colors indicate the conservatory index (CI) for each position, from the most conserved (blue CI = 0) to the least conserved positions (pink CI ≥ 0.15)(Li et al., 2013). Visualization software: PyMOL V1.5 (http://www.pymol.org/).

(C) Prevalence of natural variations at 116 Rev positions of HIV-1 group M (subtypes: A1, B, C, D, G and CRF01_AE, CRF02_AG). HXB2 indices are shown on top of the colored bars. Identified nanobody interaction positions are marked with red stars. Consensus subtype B amino acid for each position is shown directly under the bar, and is highlighted in green when the consensus amino acid differed in one or more subtypes. Natural polymorphisms are

shown below the consensus subtype B amino acids; proportions (%) are colored blue for proportion ≥ 5%; orange otherwise.

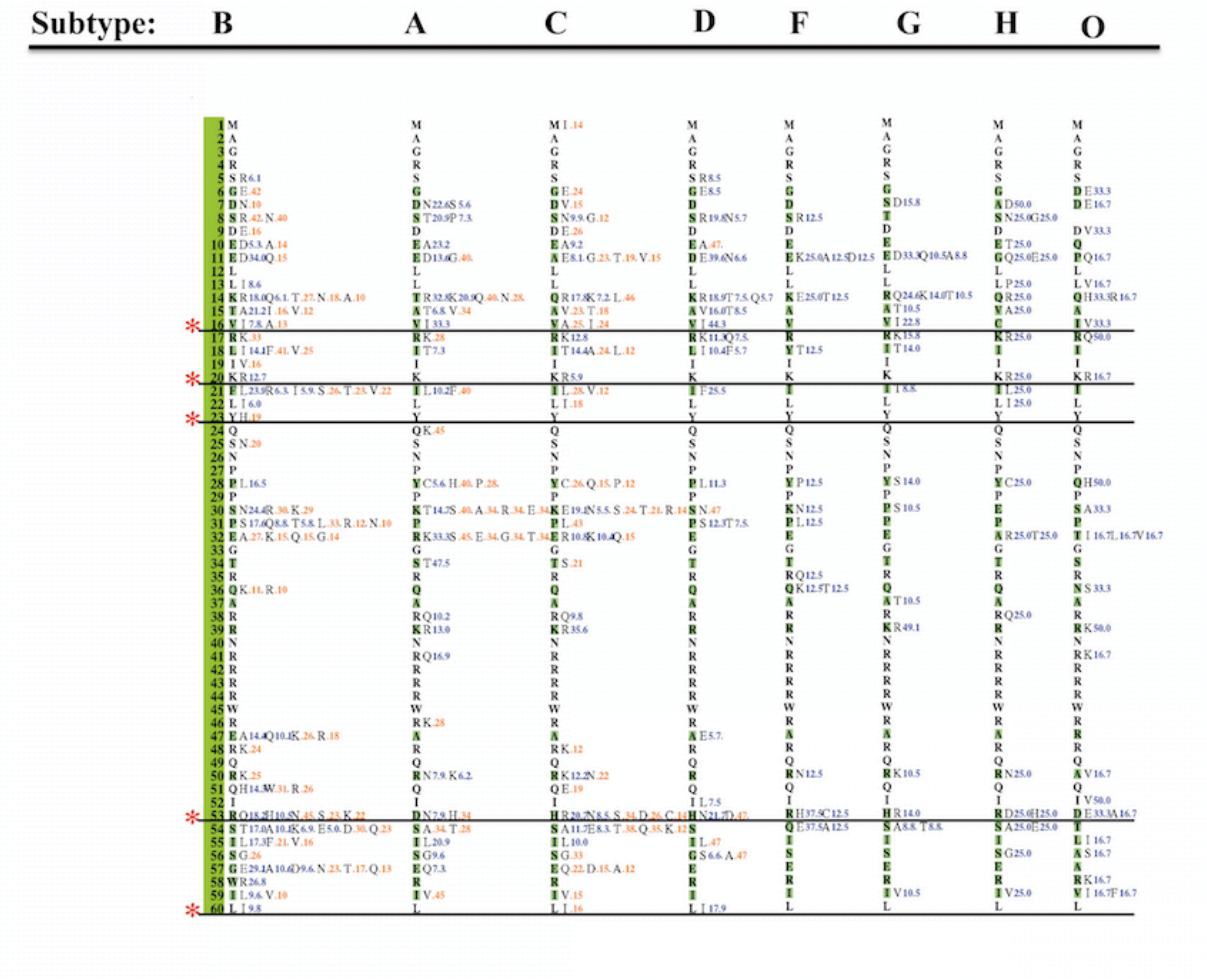

Fig. 8 Consensus sequences of different subtypes and groups

This figure shows the distribution of HIV-1 Rev natural polymorphisms within each individual subtype. HXB2 indices at each individual protein are shown in the first column, followed by HXB2 indices in the full-length Rev. Protein interaction positions are marked with red stars. The remaining columns list the consensus amino acid for each subtype followed by its natural variation(s) and the corresponding proportion(s) in blue (prevalence above 5%) and orange (prevalence at or below 5%). The amount of strains evaluated for each subtype are as follows: A (n = 177), B (n = 2701), C (n = 1027), D (n = 106), F (n = 33), G (n = 57), H (n=4), group O (n=6).

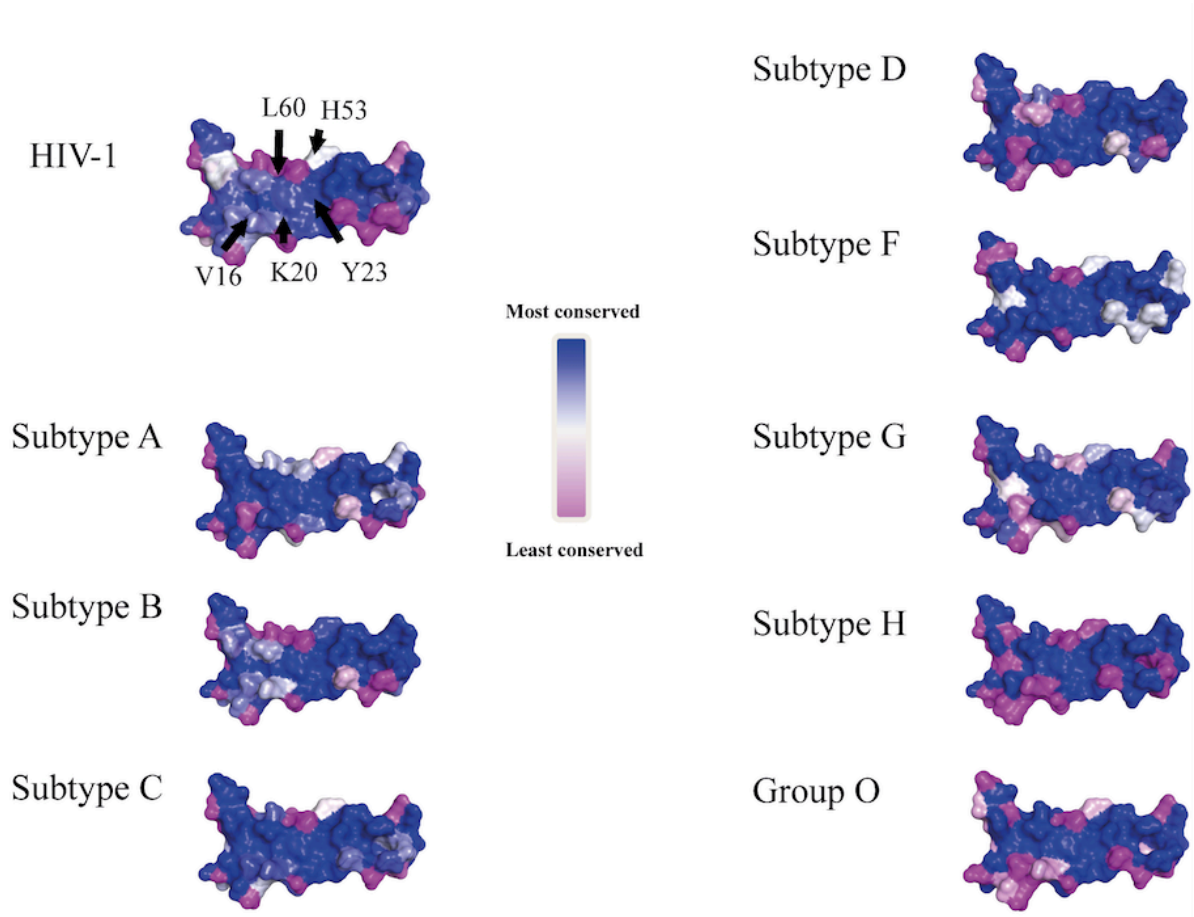

Fig. 9 Surface representation of Rev amino acid conservation in different HIV-1 subtypes

Surface spectrum colors indicate the CI at each position, from the most conserved (blue CI = 0) to the least conserved positions (pink CI ≥ 0.15). Visualization software: PyMOL V1.5 (http://www.pymol.org/).

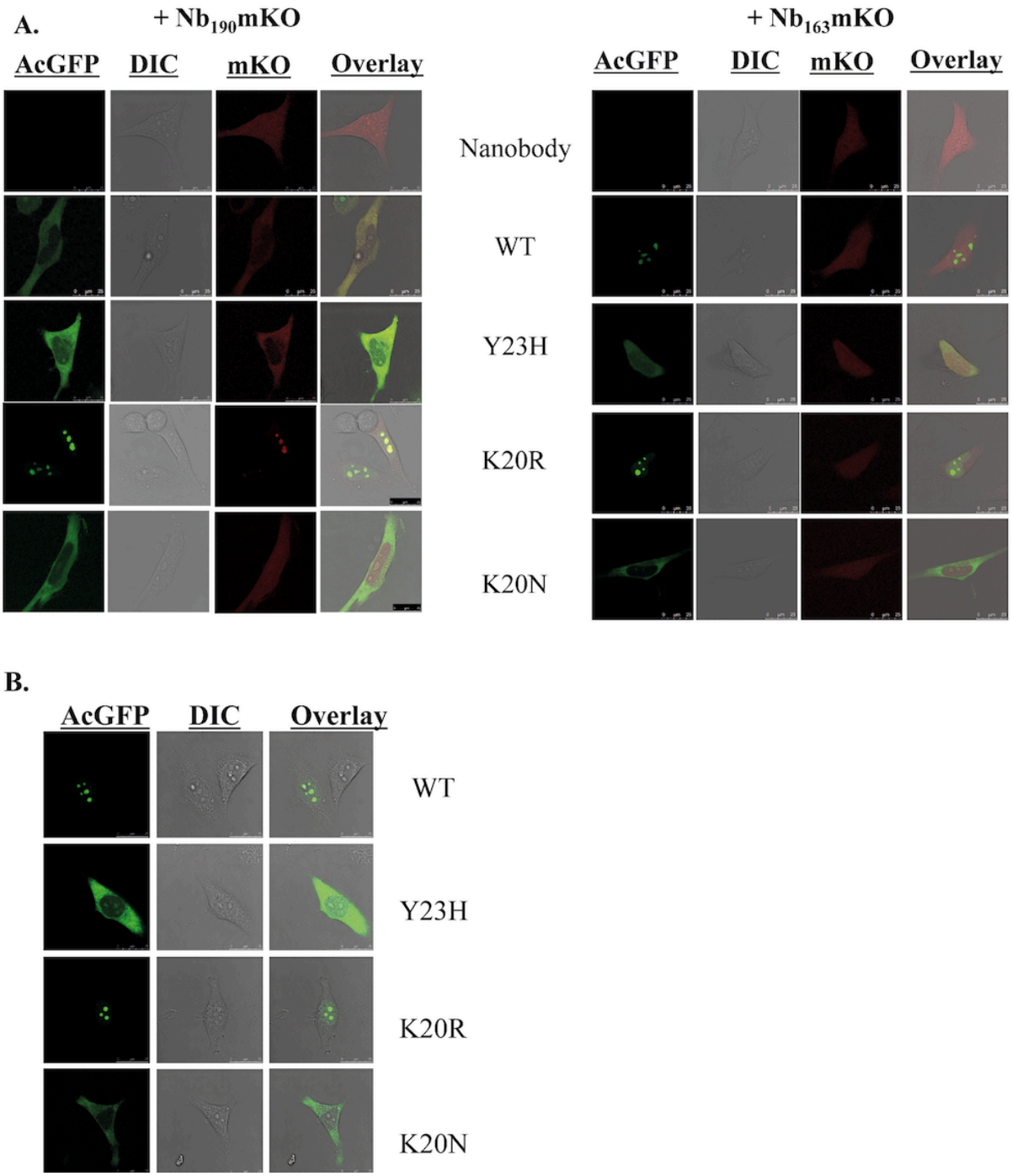

Fig. 10 Redistribution of Rev-AcGFP mutants in the presence of Nb_{190}-mKO

(A) HeLa cells were co-transfected with Rev-AcGFP together with active Nb_{190}-mKO or the negative control Nb_{163}-mKO. GFP (green) and mKO (red) were visualized by confocal fluorescence microscopy. The third column shows differential interference contrast (DIC) images.

(**B)** HeLa cells were transfected with different Rev mutants fused to AcGFP. GFP (green) was visualized using confocal fluorescence microscopy. The second column shows differential interference contrast (DIC) images.

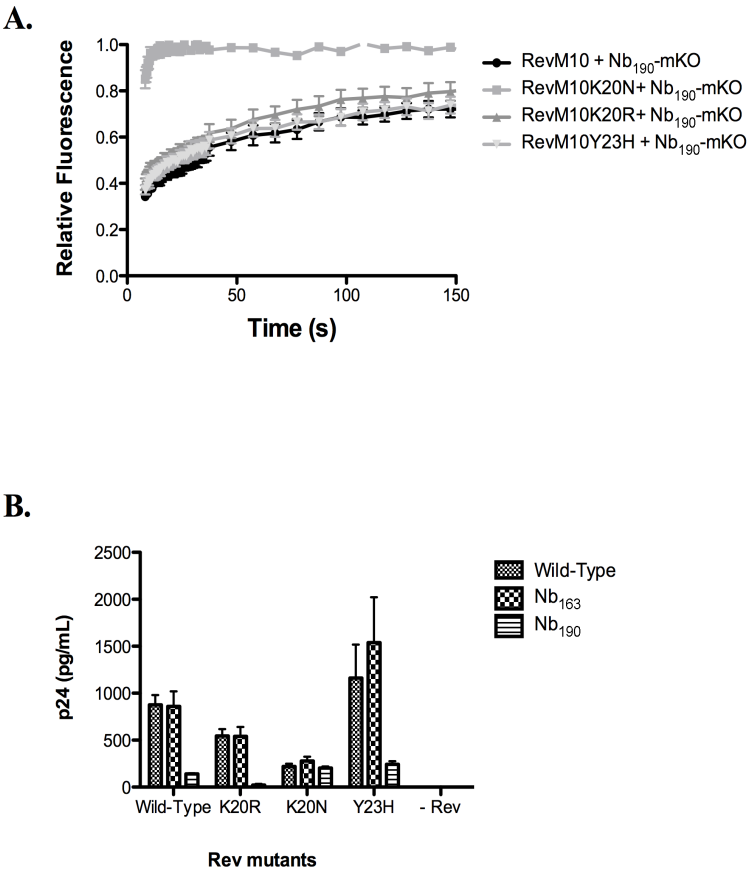

Fig. 11 Affinity of Nb_{190} for K20 or Y23 Rev mutants and effect of Nb_{190} on virus production in presence of these mutants

(A) Fluorescence Recovery after Photobleaching (FRAP) of Nb_{190} interaction with the RevM10 mutant. Relative affinity of the Rev mutants was determined by FRAP of Nb_{190}-mKO when bound to RevM10GFP. Values are averages ± SEM ($n \geq 9$)

(B) Wild-type HeLa P4 cells or HeLa P4 stably expressing Nb_{190} or Nb_{163} were co-transfected with Rev-deficient NL4.3 and mutants of Rev. Virus production from the Rev-deficient NL4.3 clone is rescued by co-expression of Rev protein. Twenty-four hours post transfection virus production was determined by monitoring the virus-associated p24 in the supernatant by ELISA. Average of 3 independent experiments with standard deviations (SD) are shown.

A.

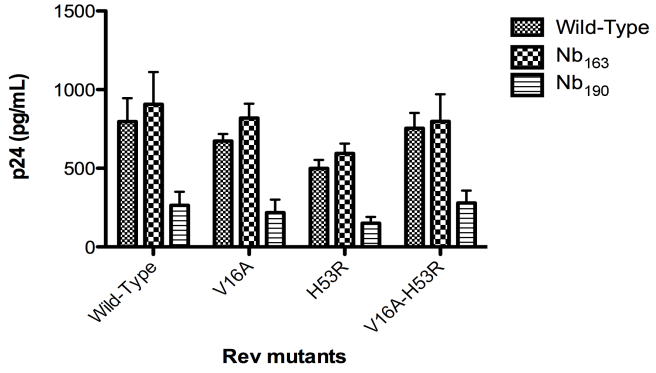

B.

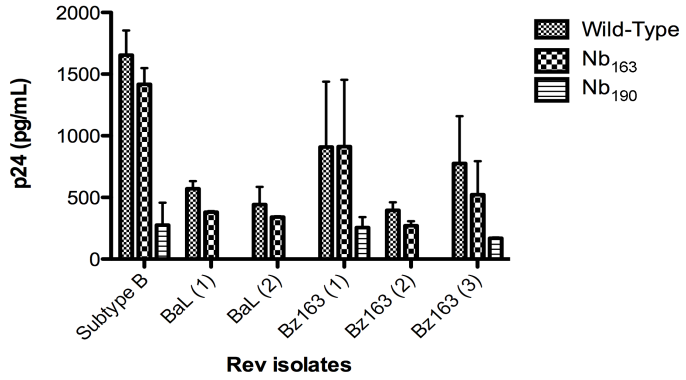

Fig. 12 Nb_{190} inhibits the function of Rev containing the V16A, H53R or double V16A-H53R mutations and of full-length Bz163 Rev

A. Wild-type HeLa P4 cells or HeLa P4 cells stably expressing Nb_{190} or Nb_{163} were co-transfected with Rev-deficient NL4.3 and mutants of Rev containing the Bz163-epitope mutations V16A, H53R, or V16AH53R. Twenty-four hours post transfection virus production was determined by monitoring the virus-associated p24 in the supernatant by ELISA. Average of 3 independent experiments with standard deviations (SD) are shown.

B. The Rev sequence of both subtype F Bz163 and subtype B BaL were cloned into an expression vector by means of reverse genetics. Three independent clones for Bz163 Rev and 2 independent clones from subtype B BaL Rev were selected. Wild-type HeLa P4 cells or HeLa P4 cells stably expressing Nb_{190} or Nb_{163} were co-transfected with Rev-deficient NL4.3

and either clones of Rev-Bz163 or Rev-BaL. Twenty-four hours post transfection virus production was determined by monitoring the virus-associated p24 in the supernatant by ELISA. As control reference NL4.3 Rev was used. Average of 3 independent experiments with standard deviations (SD) are shown.

Tables

Table 1. The inter- and intra-subtype diversity of HIV-1 Rev amino acid sequences (%)

		HIV-1 group M											Group N	Group O	Group P
		B	**A1**	**C**	**D**	**F1**	**G**	**H**	**J**	**K**	**01_AE**	**02_AG**			
Intra-diversity	**B**	0.18	0.17	0.16	0.15	0.15	0.17	0.20	0.07	0.23	0.13	0.15	0.12	0.22	0.12
Inter-diversity	**A1**		0.27	0.32	0.22	0.26	0.26	0.28	0.29	0.31	0.28	0.26	0.39	0.57	0.58
	C			0.26	0.25	0.25	0.22	0.25	0.22	0.3	0.22	0.21	0.38	0.55	0.56
	D				0.29	0.26	0.26	0.31	0.26	0.32	0.28	0.26	0.4	0.55	0.56
	F1					0.23	0.24	0.27	0.27	0.29	0.27	0.25	0.4	0.56	0.58
	G						0.23	0.26	0.23	0.26	0.24	0.23	0.38	0.55	0.54
	H							0.25	0.25	0.28	0.21	0.21	0.36	0.56	0.57
	J								0.26	0.32	0.26	0.25	0.37	0.55	0.58
	K									0.27	0.26	0.24	0.4	0.56	0.57
	01_AE										0.31	0.28	0.41	0.57	0.57
	02_AG											0.2	0.36	0.56	0.58
	N												0.36	0.55	0.58
	O													0.55	0.56
	P														0.55

Using the amino acid sequences collected from HIV-1 subtype A1, B, C, D, F1, G, H, J, K, CRF01_AE, CRF02_AG, group O, N and P (see methods), we performed pairwise sequence comparison to measure the genetic diversity within each subtype, CRF or group dataset (so-called: intra-diversity), as well as the genetic diversity between two different subtype, CRF or group datasets (so-called inter-diversity).

Table 2. Fold inhibition of different subtypes

Subtype	**A**	**B**	**B**	**C**	**D**	**F**	**G**	**H**	**O**
Virus	UG275	III_B	BaL	ETH2220	UG270	Bz163	BcFDioum	BcFKita	BcF06
Fold inhibition	>10	>100 000	>10 000	>100	>10 000	≤1	>100	> 10 000	>10

Relative inhibitory activity of Nb_{190} as compared to the effect of Nb_{163} for different subtypes calculated as the ratio of the maximum p24 values in Nb_{190}-expressing cells on p24 values in Nb_{163}-expressing cells at the same MOI measured at day 5 post infection. For BcF06 the fold inhibition was determined by calculating the ratio of 50% cell culture infective dose ($CCID_{50}$) determined by titration using the MTT method at day 5 post infection.

Table 3. Amino acid sequence of the Rev epitope residues in different HIV-1 subtypes

		V16	**K20**	**Y23**	**H53**	**L60**
Subtype A	UG275	**I**	K	Y	**D**	L
Subtype B	III_B	V	K	Y	H	L
	BaL	V	K	Y	**R**	L
Subtype C	ETH2220	V	K	Y	H	L
Subtype D	UG270	V	K	Y	H	L
Subtype F	Bz 163	**A**	K	Y	**R**	L
Subtype G	BcFDioum	V	K	Y	**D**	L
Subtype H	BcF Kita	V	K	Y	**D**	L
Subtype O	BcF06	**I**	K	Y	**D**	L

Sequences of different strains of different clades at positions V16, K20, Y23, H53 and L60 are shown. When compared to wild-type NL4.3, residue substitutions occurring in the different strains are indicated in bold; amino acids depicted in black are the same as in NL4.3.

Authors' contributions

EB, EV, TV, GL and DD designed the experiments. EB, EV and GL carried out the experiments. EB, GL and DD wrote the manuscript. EV, TV, CP and A-MV provided critical input on the manuscript and participated in discussions. All authors read and approved the final manuscript.

Disclosure of interests

The authors declare they have no competing interests.

Acknowledgements

We thank L. Bral for help in the construction of the plasmids required to establish the stable cell lines, Y. Schrooten for handling of the sequencing and K. Erven and C. Heens for MOI determination of the different HIV-strains. EB is supported by an IWT (agency for innovation through science and technology) grant. AV received funding from the Fonds voor Wetenschappelijk Onderzoek – Flanders (FWO), grant G069214N.

References

Abecasis, A.B., Wensing, A.M., Paraskevis, D., Vercauteren, J., Theys, K., Van de Vijver, D.A., Albert, J., Asjo, B., Balotta, C., Beshkov, D., Camacho, R.J., Clotet, B., De Gascun, C., Griskevicius, A., Grossman, Z., Hamouda, O., Horban, A., Kolupajeva, T., Korn, K., Kostrikis, L.G., Kucherer, C., Liitsola, K., Linka, M., Nielsen, C., Otelea, D., Paredes, R., Poljak, M., Puchhammer-Stockl, E., Schmit, J.C., Sonnerborg, A., Stanekova, D., Stanojevic, M., Struck, D., Boucher, C.A., Vandamme, A.M., 2013. HIV-1 subtype distribution and its demographic determinants in newly diagnosed patients in Europe suggest highly compartmentalized epidemics. Retrovirology 10, 7.

Anderson, J., Akkina, R., 2008. Human immunodeficiency virus type 1 restriction by human-rhesus chimeric tripartite motif 5alpha (TRIM 5alpha) in CD34(+) cell-derived macrophages in vitro and in T cells in vivo in severe combined immunodeficient (SCID-hu) mice transplanted with human fetal tissue. Human gene therapy 19, 217-228.

Barre-Sinoussi, F., Ross, A.L., Delfraissy, J.F., 2013. Past, present and future: 30 years of HIV research. Nature reviews. Microbiology.

Bray, M., Prasad, S., Dubay, J.W., Hunter, E., Jeang, K.T., Rekosh, D., Hammarskjold, M.L., 1994. A small element from the Mason-Pfizer monkey virus genome makes human immunodeficiency virus type 1 expression and replication Rev-independent. Proceedings of the National Academy of Sciences of the United States of America 91, 1256-1260.

Callewaert, F., Roodt, J., Ulrichts, H., Stohr, T., van Rensburg, W.J., Lamprecht, S., Rossenu, S., Priem, S., Willems, W., Holz, J.B., 2012. Evaluation of efficacy and safety of the anti-VWF Nanobody ALX-0681 in a preclinical baboon model of acquired thrombotic thrombocytopenic purpura. Blood 120, 3603-3610.

Daelemans, D., Costes, S.V., Cho, E.H., Erwin-Cohen, R.A., Lockett, S., Pavlakis, G.N., 2004. In vivo HIV-1 Rev multimerization in the nucleolus and cytoplasm identified by fluorescence resonance energy transfer. J Biol Chem 279, 50167-50175.

Daelemans, D., Costes, S.V., Lockett, S., Pavlakis, G.N., 2005. Kinetic and molecular analysis of nuclear export factor CRM1 association with its cargo in vivo. Molecular and cellular biology 25, 728-739.

Daly, T.J., Cook, K.S., Gray, G.S., Maione, T.E., Rusche, J.R., 1989. Specific binding of HIV-1 recombinant Rev protein to the Rev-responsive element in vitro. Nature 342, 816-819.

Daugherty, M.D., D'Orso, I., Frankel, A.D., 2008. A solution to limited genomic capacity: using adaptable binding surfaces to assemble the functional HIV Rev oligomer on RNA. Molecular cell 31, 824-834.

Daugherty, M.D., Liu, B., Frankel, A.D., 2010. Structural basis for cooperative RNA binding and export complex assembly by HIV Rev. Nature structural & molecular biology 17, 1337-1342.

DiMattia, M.A., Watts, N.R., Stahl, S.J., Rader, C., Wingfield, P.T., Stuart, D.I., Steven, A.C., Grimes, J.M., 2010. Implications of the HIV-1 Rev dimer structure at 3.2 A resolution

for multimeric binding to the Rev response element. Proceedings of the National Academy of Sciences of the United States of America 107, 5810-5814.

Fischer, U., Huber, J., Boelens, W.C., Mattaj, I.W., Luhrmann, R., 1995. The HIV-1 Rev activation domain is a nuclear export signal that accesses an export pathway used by specific cellular RNAs. Cell 82, 475-483.

Fischer, U., Pollard, V.W., Luhrmann, R., Teufel, M., Michael, M.W., Dreyfuss, G., Malim, M.H., 1999. Rev-mediated nuclear export of RNA is dominant over nuclear retention and is coupled to the Ran-GTPase cycle. Nucleic acids research 27, 4128-4134.

Gouy, M., Guindon, S., Gascuel, O., 2010. SeaView version 4: A multiplatform graphical user interface for sequence alignment and phylogenetic tree building. Molecular biology and evolution 27, 221-224.

Heaphy, S., Dingwall, C., Ernberg, I., Gait, M.J., Green, S.M., Karn, J., Lowe, A.D., Singh, M., Skinner, M.A., 1990. HIV-1 regulator of virion expression (Rev) protein binds to an RNA stem-loop structure located within the Rev response element region. Cell 60, 685-693.

Hemelaar, J., Gouws, E., Ghys, P.D., Osmanov, S., Isolation, W.-U.N.f.H., Characterisation, 2011. Global trends in molecular epidemiology of HIV-1 during 2000-2007. Aids 25, 679-689.

Holz, J.B., 2012. The TITAN trial--assessing the efficacy and safety of an anti-von Willebrand factor Nanobody in patients with acquired thrombotic thrombocytopenic purpura. Transfusion and apheresis science : official journal of the World Apheresis Association : official journal of the European Society for Haemapheresis 46, 343-346.

Jain, C., Belasco, J.G., 2001. Structural model for the cooperative assembly of HIV-1 Rev multimers on the RRE as deduced from analysis of assembly-defective mutants. Molecular cell 7, 603-614.

Kalland, K.H., Szilvay, A.M., Brokstad, K.A., Saetrevik, W., Haukenes, G., 1994. The human immunodeficiency virus type 1 Rev protein shuttles between the cytoplasm and nuclear compartments. Molecular and cellular biology 14, 7436-7444.

Li, G., Verheyen, J., Rhee, S.Y., Voet, A., Vandamme, A.M., Theys, K., 2013. Functional conservation of HIV-1 Gag: implications for rational drug design. Retrovirology 10, 126.

Malim, M.H., Cullen, B.R., 1991. HIV-1 structural gene expression requires the binding of multiple Rev monomers to the viral RRE: implications for HIV-1 latency. Cell 65, 241-248.

Malim, M.H., Hauber, J., Le, S.Y., Maizel, J.V., Cullen, B.R., 1989. The HIV-1 rev trans-activator acts through a structured target sequence to activate nuclear export of unspliced viral mRNA. Nature 338, 254-257.

McNally, J.G., 2008. Quantitative FRAP in analysis of molecular binding dynamics in vivo. Methods in cell biology 85, 329-351.

Meyer, B.E., Malim, M.H., 1994. The HIV-1 Rev trans-activator shuttles between the nucleus and the cytoplasm. Genes & development 8, 1538-1547.

Muyldermans, S., Cambillau, C., Wyns, L., 2001. Recognition of antigens by single-domain antibody fragments: the superfluous luxury of paired domains. Trends in biochemical sciences 26, 230-235.

Neville, M., Stutz, F., Lee, L., Davis, L.I., Rosbash, M., 1997. The importin-beta family member Crm1p bridges the interaction between Rev and the nuclear pore complex during nuclear export. Current biology : CB 7, 767-775.

Oliveira, S., Heukers, R., Sornkom, J., Kok, R.J., van Bergen En Henegouwen, P.M., 2013. Targeting tumors with nanobodies for cancer imaging and therapy. Journal of controlled release : official journal of the Controlled Release Society 172, 607-617.

Pannecouque, C., Daelemans, D., De Clercq, E., 2008. Tetrazolium-based colorimetric assay for the detection of HIV replication inhibitors: revisited 20 years later. Nature protocols 3, 427-434.

Pardon, E., Laeremans, T., Triest, S., Rasmussen, S.G., Wohlkonig, A., Ruf, A., Muyldermans, S., Hol, W.G., Kobilka, B.K., Steyaert, J., 2014. A general protocol for the generation of Nanobodies for structural biology. Nature protocols 9, 674-693.

Pauwels, R., Balzarini, J., Baba, M., Snoeck, R., Schols, D., Herdewijn, P., Desmyter, J., De Clercq, E., 1988. Rapid and automated tetrazolium-based colorimetric assay for the detection of anti-HIV compounds. Journal of virological methods 20, 309-321.

Pineda-Pena, A.C., Faria, N.R., Imbrechts, S., Libin, P., Abecasis, A.B., Deforche, K., Gomez-Lopez, A., Camacho, R.J., de Oliveira, T., Vandamme, A.M., 2013. Automated subtyping of HIV-1 genetic sequences for clinical and surveillance purposes: Performance evaluation of the new REGA version 3 and seven other tools. Infection, genetics and evolution : journal of molecular epidemiology and evolutionary genetics in infectious diseases 19, 337-348.

Pollard, V.W., Malim, M.H., 1998. The HIV-1 Rev protein. Annual review of microbiology 52, 491-532.

Rose, P.P., Korber, B.T., 2000. Detecting hypermutations in viral sequences with an emphasis on G --> A hypermutation. Bioinformatics 16, 400-401.

Siontorou, C.G., 2013. Nanobodies as novel agents for disease diagnosis and therapy. International journal of nanomedicine 8, 4215-4227.

Sodroski, J., Goh, W.C., Rosen, C., Dayton, A., Terwilliger, E., Haseltine, W., 1986. A second post-transcriptional trans-activator gene required for HTLV-III replication. Nature 321, 412-417.

Sonigo, P., Barker, C., Hunter, E., Wain-Hobson, S., 1986. Nucleotide sequence of Mason-Pfizer monkey virus: an immunosuppressive D-type retrovirus. Cell 45, 375-385.

Stahl, S.J., Watts, N.R., Rader, C., DiMattia, M.A., Mage, R.G., Palmer, I., Kaufman, J.D., Grimes, J.M., Stuart, D.I., Steven, A.C., Wingfield, P.T., 2010. Generation and characterization of a chimeric rabbit/human Fab for co-crystallization of HIV-1 Rev. Journal of molecular biology 397, 697-708.

Thomas, S.L., Oft, M., Jaksche, H., Casari, G., Heger, P., Dobrovnik, M., Bevec, D., Hauber, J., 1998. Functional analysis of the human immunodeficiency virus type 1 Rev protein oligomerization interface. Journal of virology 72, 2935-2944.

Ulm, J.W., Perron, M., Sodroski, J., R, C.M., 2007. Complex determinants within the Moloney murine leukemia virus capsid modulate susceptibility of the virus to Fv1 and Ref1-mediated restriction. Virology 363, 245-255.

Venken, T., Daelemans, D., De Maeyer, M., Voet, A., 2012. Computational investigation of the HIV-1 Rev multimerization using molecular dynamics simulations and binding free energy calculations. Proteins 80, 1633-1646.

Vercruysse, T., Boons, E., Venken, T., Vanstreels, E., Voet, A., Steyaert, J., De Maeyer, M., Daelemans, D., 2013. Mapping the binding interface between an HIV-1 inhibiting intrabody and the viral protein Rev. PLoS One 8, e60259.

Vercruysse, T., Daelemans, D., 2014. HIV-1 Rev Multimerization: Mechanism and Insights. Current HIV research.

Vercruysse, T., Pardon, E., Vanstreels, E., Steyaert, J., Daelemans, D., 2010. An intrabody based on a llama single-domain antibody targeting the N-terminal alpha-helical multimerization domain of HIV-1 rev prevents viral production. J Biol Chem 285, 21768-21780.

Vercruysse, T., Pawar, S., De Borggraeve, W., Pardon, E., Pavlakis, G.N., Pannecouque, C., Steyaert, J., Balzarini, J., Daelemans, D., 2011. Measuring cooperative Rev protein-protein interactions on Rev responsive RNA by fluorescence resonance energy transfer. RNA Biol 8, 316-324.

Zapp, M.L., Hope, T.J., Parslow, T.G., Green, M.R., 1991. Oligomerization and RNA binding domains of the type 1 human immunodeficiency virus Rev protein: a dual function for an arginine-rich binding motif. Proceedings of the National Academy of Sciences of the United States of America 88, 7734-7738.

Zhen, A., Kitchen, S., 2014. Stem-cell-based gene therapy for HIV infection. Viruses 6, 1-12.

Zolotukhin, A.S., Valentin, A., Pavlakis, G.N., Felber, B.K., 1994. Continuous propagation of RRE(-) and Rev(-)RRE(-) human immunodeficiency virus type 1 molecular clones containing a cis-acting element of simian retrovirus type 1 in human peripheral blood lymphocytes. Journal of virology 68, 7944-7952.